Quantifying the tuneable interactions between colloid supported lipid bilayers

Emma C. Giakoumatos[1,2,3], Berta Gumí Audenis[1,3], Álvaro González García[2,3], Laura S. van Hazendonk[2,3], Heiner Friedrich[2,3], Remco Tuinier[2,3] and Ilja K. Voets[1,3]*

[1]Laboratory of Self-Organizing Soft Matter, Department of Chemical Engineering and Chemistry, Eindhoven University of Technology, Eindhoven, Netherlands, [2]Laboratory of Physical Chemistry, Department of Chemical Engineering and Chemistry, Eindhoven University of Technology, Eindhoven, Netherlands, [3]Institute for Complex Molecular Systems (ICMS), Eindhoven University of Technology, Eindhoven, Netherlands

Colloid supported lipid bilayers (CSLBs) are formed *via* the rupture and fusion of lipid vesicles to coat spherical colloidal particles. CSLBs are an emerging vector for the controlled self-assembly of colloids due to the ability to include additives into the bilayer, which influence the (a)specific interactions between particles. To evaluate the specificity of CSLB assembly, first a fundamental study on the tunability of the colloidal interaction and resulting colloidal stability of CSLBs without specific interactions is reported here. It was found that both fluid and gel CSLBs showed significant clustering and attraction, while the addition of steric stabilizers induced a profound increase in stability. The interactions were rendered attractive again by the introduction of depletion forces *via* the addition of free non-adsorbing polymers. The compositions of fluid and gel CSLBs with 5% membrane stabiliser were concluded to be optimal for further studies where both colloidal stability, and contrasting membrane fluidity are required. These experimental findings were confirmed semi-quantitatively by predictions using numerical self-consistent mean-field theory lattice computations.

KEYWORDS

colloid supported lipid bilayers, colloidal interactions, clustering, depletion interaction, membrane fluidity, radial distribution function, self-consistent field theory

Introduction

Colloidal dispersions are ubiquitous in the field of material science as components of industrial products such as coatings and pharmaceuticals, in models for biological systems, and in experimental studies such as those on colloidal self-assembly to create complex architectures (Poon et al., 1996; Anderson and Lekkerkerker, 2002; Lu et al., 2008). For a colloidal dispersion to be stable, the particles must on average be spatially well distributed and/or existing primarily as single particles rather than clusters. For example, repulsive particles tend to avoid short distances between one another, while in attractive systems the particles tend to be clustered. In attractive systems the probability of particles to be close to one another is enhanced if the attraction is weak, while aggregation of particles is observed when the attraction is strong (Poon et al., 1996; Anderson and Lekkerkerker, 2002; Lu et al., 2008). Therefore, the non-randomness of the relative position of particles in a dispersion is caused by interactions between them, such as excluded volume, van der Waals, electrostatic and polymer mediated interactions (Yethiraj and van Blaaderen, 2003; Lu et al., 2008).

Colloid supported lipid bilayers (CSLBs) are designed by coating colloidal particles with lipid bilayers. The modular approach to producing CSLBs makes it possible to tune their surface chemistry, membrane fluidity, and interparticle interactions through adjustments in bilayer composition. The tendency of CSLBs to self-assemble, for example, is dependent on the inclusion into the bilayer of PEGylated lipids or (im)mobile linkers, such as DNA, with specific binding properties (Yethiraj and van Blaaderen, 2003; van der Meulen and Leunissen, 2013; van der Meulen et al., 2015; Chakraborty et al., 2017; Moerman, 2019; Rinaldin et al., 2019). To create responsive materials from such CSLBs with membranes that can switch between a fluid and non-fluid state without uncontrolled aggregation, it is helpful to identify a range of membrane compositions where colloidal stability is maximised and to assess the modulation of the effective interaction between CSLBs of each of the incorporated membrane additives (Needham and Kim, 2000; Garbuzenko et al., 2005; van der Meulen and Leunissen, 2013; van der Meulen et al., 2015; Rinaldin et al., 2020). For example, including increasing amounts of a PEGylated lipid into CSLBs comprised of a fluid membrane has been previously shown to enhance the number of single CSLBs in a dispersion (Rinaldin et al., 2019). However, a quantitative investigation on the strength of the aspecific interactions is yet to be completed (Rinaldin et al., 2019). Here, we would like to compare to and expand on this previous work by quantitatively examining the spatial distribution of CSLBs comprised of fluid and gel bilayers, and by studying the influence of PEGylated lipids on membrane stability. Additionally, the tunability of the colloidal system is further examined by destabilising the system through addition of a non-adsorbing polymer depletant (de Hoog et al., 2001; Lekkerkerker and Tuinier, 2011a; Whitmer and Luijten, 2011). Using confocal microscopy, we study and characterise colloidal dispersions in real space and time on the particle level.

The focus of this investigation is to quantitatively assess the colloidal interactions of CSLBs using two approaches: analysis of the cluster size distribution, and the indirect quantification of CSLB pair interactions *via* the calculation of radial distribution functions, $g(r)$ (Bergman, 2019). Here, r is the distance from the centre of a particle. In a colloidal dispersion the local particle density $\rho(r)$, is related to the average particle density, $\bar{\rho}$ by (Royall et al., 2003; Yethiraj and van Blaaderen, 2003; Bergman, 2019):

$$\rho(r) = \bar{\rho}g(r). \qquad (1)$$

Hence $g(r \rightarrow \infty) = 1$. For particles with an excluded volume core, $g(r < d) = 0$ where d is the sphere diameter. Close to this value, a sharp first peak occurs, indicating the probability of finding a particle directly next to the central particle (Hill, 1986; Royall et al., 2003; Yethiraj and van Blaaderen, 2003; Bergman, 2019; Ivell et al., 2013). Furthermore, in the limit of a dilute colloidal suspension, the pair interaction between particles is given by:

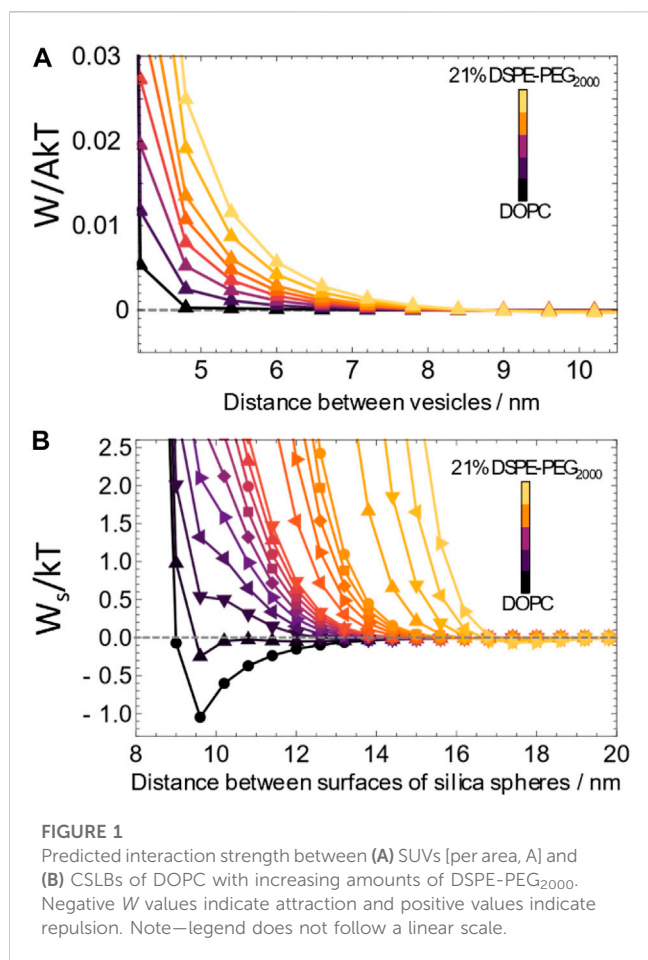$$g(r) = e^{-\frac{W(r)}{kT}}, \qquad (2)$$

where $W(r)$ is the pair potential, k is Boltzmann's constant and T is the temperature (Hill, 1986). For non-dilute systems Eq. 2 still holds, however $W(r)$ is then replaced by the potential of mean force $W_{PMF}(r)$. The potential mean force is affected not only by the pair interactions but also by many body interactions and hence

the particle concentration. For dispersions of equivalent particle concentrations, the relative height of the first peak can be used to compare the strength of interaction, where a higher peak indicates a stronger inter-particle attraction (Eq. 2). In systems where strong interactions are present, or high particle concentrations are examined, additional peaks may be present at r values approximately corresponding to multiples of the particle diameter (Hill, 1986; Royall et al., 2003; Yethiraj and van Blaaderen, 2003; Bergman, 2019; Ivell et al., 2013). Numerical lattice computations based upon self-consistent mean-field theory (SCFT) were utilised in a previous study to elucidate the spatial composition of small unilamellar vesicles (SUVs) and CSLBs (Giakoumatos et al., 2022).

The SCFT method employed here is based upon (Scheutjens and Fleer, 1979; Scheutjens and Fleer, 1980; Fleer et al., 1993) a Flory–Huggins-like lattice theory, using Flory–Huggins interaction parameters and a small systems thermodynamics approach (Leermakers et al., 2005). The SCFT method goes beyond Flory–Huggins in the sense that it enables us to account for inhomogeneities (concentration gradients) of all compounds (Fleer, 2010). When charges are involved (Leermakers et al., 2005; Lauw et al., 2006) the SCFT computations solve the full Poisson equation (on a mean-field level) for finitely sized ions and solvent molecules. SCFT computations yield, e.g., electrostatic potential, chemical potentials, the free energy of the system, allowing the description of self-assembly, for example, by predicting the size, morphology and local density profiles. By changing the distance between objects the free energy of interaction can be determined (Fleer, 2010; Philipse et al., 2017; González García et al., 2020). In our previous paper (Giakoumatos et al., 2022), we have applied SCFT to predict some thermodynamic properties of SUVs and CSLBs, by following the work of Meijer, Leermakers and Lyklema as starting point (Meijer et al., 1995). Herein SCFT is applied to predict the nature and strength of interactions (W) between SUVs and between CSLBs at equilibrium (Li et al., 2009; Ianiro et al., 2018; González García et al., 2019; Ianiro et al., 2019; González García et al., 2020).

Results and discussion

In this investigation we aim to identify the optimum CSLB membrane composition for colloidal stability and to quantify the degree to which the interactions between CSLBs can be modulated. First, the type and strength of interaction between colloid supported lipid bilayers of DOPC and their unsupported counterparts (in the form of small unilamellar vesicles, SUVs) with and without (2 kDa) PEGylated lipid stabiliser are predicted theoretically. Next, we image CSLBs of 3 μm in diameter (in 10 mM HEPES with 50 mM NaCl) with fluid and gel phospholipids, and with varying amounts of PEGylated lipids and added depletants, at multiple particle concentrations in real space and time on the particle level by confocal microscopy. Finally, we assess the impact of membrane fluidity, stabilizers and depletants on colloidal stability through analysis of the CSLB cluster distribution and a comparison of the corresponding $g(r)$.

FIGURE 1
Predicted interaction strength between **(A)** SUVs [per area, A] and
(B) CSLBs of DOPC with increasing amounts of DSPE-PEG$_{2000}$.
Negative W values indicate attraction and positive values indicate
repulsion. Note—legend does not follow a linear scale.

Theoretical prediction of the interactions between CSLBs and impact of PEGylated lipid

To begin SCFT is used to predict the nature and strength of interactions (W) between SUVs and between CSLBs at equilibrium (ESI—Supplementary Section S1). (Li et al., 2009; Ianiro et al., 2018; González García et al., 2019; Ianiro et al., 2019; González García et al., 2020) As a representative case, the interaction between SUVs and between CSLBs composed of fluid lipid 1,2-dioleoyl-sn-glycero-3-phosphocholine (DOPC) with and without membrane additive poly (ethylene glycol) (PEG)-conjugated lipid 1,2-distearoyl-sn-glycero-3-phosphoethanolamine-N-[methoxy (polyethylene glycol)-2000] (DSPE-PEG$_{2000}$) were predicted as a function of surface-to-surface distance (Figure 1). The interactions accounted for in the SCFT computations employed are direct interactions between all components quantified through Flory-Huggins parameters and electrostatic ones. The electrostatics are described using Gouy-Chapman equations (combining Boltzmann for the distribution of charges plus Poisson's equation, see Ref 24 and ESI—Supplementary Section S1 for further information).

Negative W values indicate interparticle distances that give rise to attractive interactions, while overall positive values are characteristic for repulsive systems which can be considered colloidally stable. The interactions between DOPC SUVs (Figure 1A) were found to be repulsive within 10 nm proximity,

regardless of the PEGylated lipid concentration. The overall repulsive interactions reflect the stability of the SUVs, which confirms what has been observed experimentally (Giakoumatos et al., 2022). Upon adding relatively more PEGylated lipids, the repulsive interaction becomes longer ranged and gets stronger (Figure 1A). Without PEGylated DSPE the repulsive interaction gets significant when the bilayers are less than 5 nm apart, while this distance increases upon adding more PEGylated DSPE. For 21% PEGylated DSPE it increases to almost 8 nm. Hence, the minimum proximity between DOPC SUVs can be seen to increase by a few nm upon addition of 2–21 mol% DSPE-PEG$_{2000}$, obviously due to an additional steric repulsion mediated by the PEG$_{2000}$ chains.

Interestingly, upon the formation of CSLBs by the rupture and fusion of DOPC bilayers onto the surface of silica spheres, an attractive well (see Figure 1B) appears at an interparticle distance of approximately 9 nm. This distance can be ascribed to the thickness of the bilayers on the respective silica spheres and suggests that DOPC CSLBs without DSPE-PEG$_{2000}$ are prone to aggregation. An attractive contribution to the interaction between such lipid bilayers was found already by Meijer, Leermakers, and Lyklema (Meijer et al., 1995). The relative strength of this attraction depends on the solvent conditions and details of the phospholipid type. It is an entropic effect caused by alteration of the head-group conformations when the two bilayers come in close contact. Compellingly, the addition of even minimal amounts of PEGylated lipid on the interactions between DOPC CSLBs is perceptible (Figure 1B). Upon the inclusion of 0.5 mol% DSPE-PEG$_{2000}$ the attractive well is seen to dissipate, with the system displaying increasingly repulsive interactions at greater PEGylated lipid concentration. Furthermore, the minimum distance between the CSLBs can be seen to significantly increase upon increasing DSPE-PEG$_{2000}$ addition, suggesting that steric repulsion is induced by the PEGylated lipid. Based on these computations, we select CSLBs with 0, 5 and 10 mol% stabilizer for confocal imaging so as to examine experimentally the stability of and interactions between CSLBs predicted to be aggregation-prone (without stabilizer) and colloidally stable (with modest amounts, 5 and 10 mol%, of DSPE-PEG$_{2000}$).

To determine whether the PEG chains are in the mushroom or brush regime we estimate the reduced PEG anchor density Σ from $\Sigma = \pi \sigma R_g^2$, with σ the anchor density and R_g the radius of gyration of a PEG chain. Using literature values for the area per lipid in the bilayer, A_L (Pyrkova et al., 2011), and the radius of gyration of PEG$_{2000}$, R_g = 1.8 nm (Devanand and Selser, 1991), we compute reduced anchor densities just below ($\Sigma_{DOPC, 5 mol\%}$ = 0.7; $\Sigma_{DPPC, 5 mol\%}$ = 0.8) and just above ($\Sigma_{DOPC, 5 mol\%}$ = 1.4; $\Sigma_{DPPC, 5 mol\%}$ = 1.7) for 5 and 10 mol% DSPE-PEG$_{2000}$ in a DOPC and DPPC membrane. The small difference between the two bilayers pertains to the slightly smaller area per lipid (and thus higher anchor density, $\sigma = A_L^{-1}$) for DPPC (A_{DPPC} = 0.614) compared to DOPC (A_{DOPC} = 0.717). This suggests that the PEG chain density is in the intermediate regime between the characteristic "mushroom" limit ($\Sigma \ll 1$) and "brush" limit ($\Sigma \gg 1$). This is in line with the shape of by SCFT computed PEG volume fraction profiles reported previously (Giakoumatos et al., 2022), which do not exhibit a clear peak as is characteristic for grafted chains deep in the mushroom regime. It is noted that a brush layer is not essential to provide significant steric repulsion. Stenkamp and Berg showed a small amount of sufficiently long
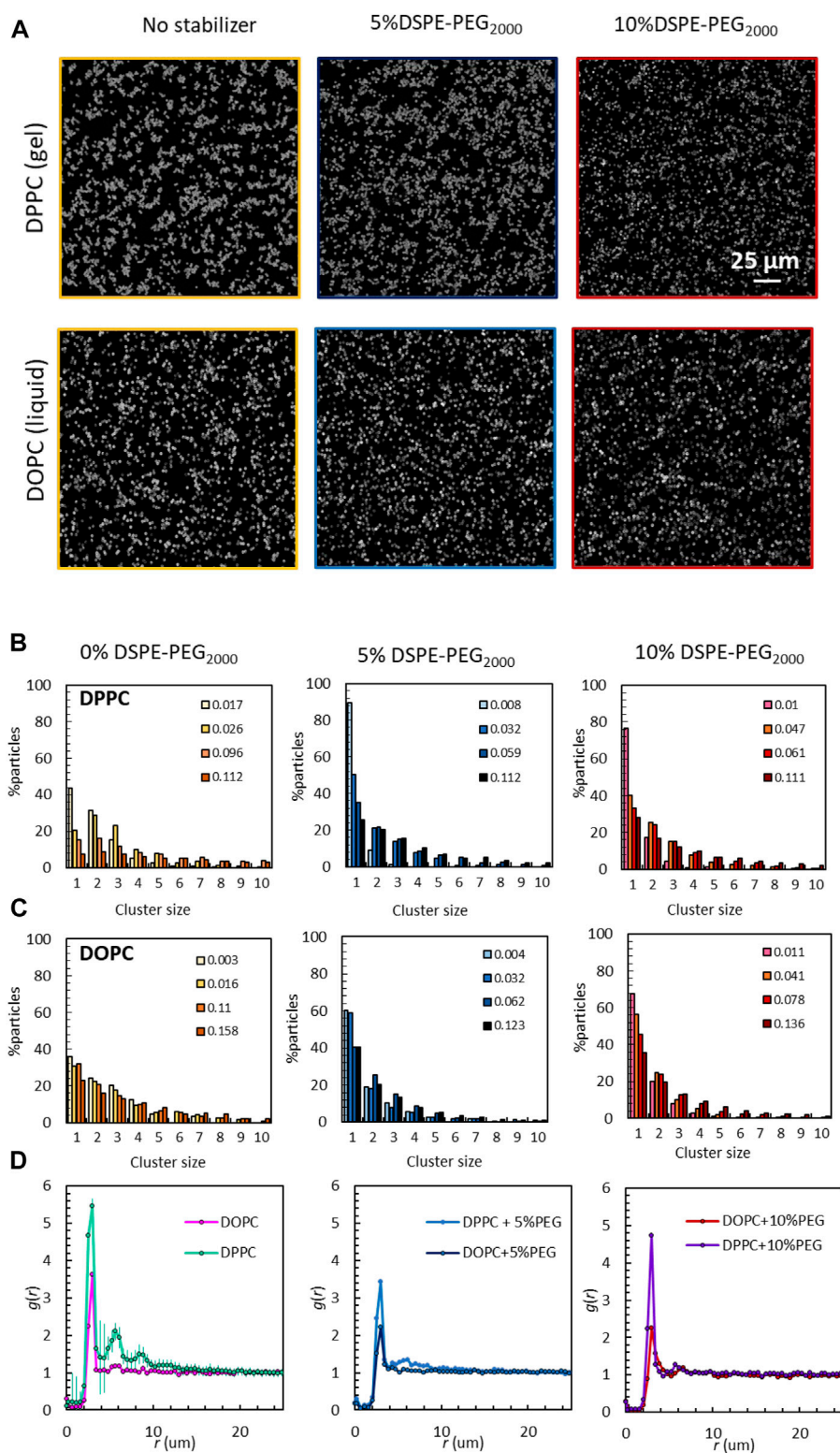
FIGURE 2
(A) confocal microscopy images of DOPC and DPPC CSLBs with 0, 5 and 10%DSPE-PEG$_{2000}$ at φ = 0.11. **(B−C)** Cluster size distribution for **(B)** DPPC CSLBs (gel) and **(C)** DOPC CSLBs (fluid) with 0 (left/yellow), 5 (middle/blue) and 10% (right/red) membrane bound DSPE-PEG$_{2000}$ for area fractions ranging from dilute to concentrated. **(D)** Comparison of probability density functions of DPPC and DOPC CSLBs at φ = 0.11 with (left panel) 0% DSPE-PEG$_{2000}$ (middle panel) 5% DSPE-PEG$_{2000}$ and (right panel) 10% DSPE-PEG$_{2000}$.

FIGURE 3
Spatial SCFT profiles predicting the interaction of 100 kDa PEG depletant at a fixed bulk PEG volume fraction of $\varphi = 10^{-4}$ (green) with **(A)** bare silica spheres, **(B)** DOPC CSLBs (black) and **(C)** DOPC + DSPE-PEG$_{2000}$ CSLBs (dashed black lines). The silica surface is indicated by the grey region. The phospholipid density profiles resulting from the SCFT computations **(B, C)** seem to suggest a thin water-rich layer of a few nm between the lipid bilayer and the bulk; the lipid concentration attains a maximum value a few nm from the silica surface.

anchored chains suffices to provide enough steric repulsion (Stenkamp and Berg, 1997).

Impact of membrane fluidity and PEGylated-lipid on CSLB interaction

To examine the CSLB interaction as a function of membrane fluidity, by comparing fluid and gel phospholipids, and as a function of the amount of bilayer-inserted PEGylated-lipids, confocal imaging was performed at multiple particle concentrations. The cluster analysis and pair interactions of the large confocal images were computed using a Matlab script relying on circle matching, segmentation and cluster assignment based on connectivity (ESI—Supplementary Section S6). The accuracy of this method to determine cluster sizes and strength of pair interactions was confirmed using a scanning electron microscopy (SEM) image of the 3 μm silica spheres used to form the CSLBs (ESI—Supplementary Figure S7). Further, it was found that the resulting $g(r)$ did not significantly depend on the value of r_{max} chosen, and so for this study r_{max} of 100 was fixed at 100 μm (ESI—Supplementary Section S8). As the measurements were completed in quasi-2D due to the tendency for the particles to sediment on the coverslip, here we report the concentration of CSLBs in terms of area fraction φ (ESI—Supplementary Section S5). The concentration of a colloidal dispersion is an important parameter in considering the system stability and potential for application and has a profound impact on the effective $g(r)$. Therefore, it is important to study the impact of many body interactions in addition to the pair interaction. To thoroughly examine this, a wide range of area fractions were tested varying from dilute to concentrated (ESI—Supplementary Figure S4). Importantly, the resulting $g(r)$ are only comparable between those samples of equivalent area fractions. For the purposes of this paper, we focus on the results of samples of relatively low ($\varphi = 0.017$) and relatively high ($\varphi = 0.11$) area fractions.

We examine the stability of and interactions between CSLBs composed of the gel phospholipid 1,2-dipalmitoyl-*sn*-glycero-3-phosphocholine (DPPC) or the fluid phospholipid DOPC, and the impact of imbedding PEGylated lipid in the bilayer. Specifically, we focus on CSLBs containing 0, 5 and 10 mol% of membrane anchored DSPE-PEG$_{2000}$. The mobility of the bilayer on the silica scaffold at each of these conditions was investigated previously using fluorescence recovery after photobleaching (FRAP) (Giakoumatos et al., 2022). It was found that the membrane of DOPC and DOPC+5%DSPE-PEG$_{2000}$ CSLBs demonstrated high fluidity, while DOPC+10%DSPE-PEG$_{2000}$ did not recover within 10 min. This is hypothesised to be due to stiffening of the bilayer [or changes in its spontaneous curvature or thermal fluctuations (Tribet and Vial, 2008)] induced by increased amounts of the high T_m phospholipid DSPE-PEG$_{2000}$ in the membrane, or the pinning of PEG to the silica scaffold surface impeding lateral movement. CSLBs consisting of DPPC as the primary lipid did not show recovery regardless of PEGylated lipid concentration.
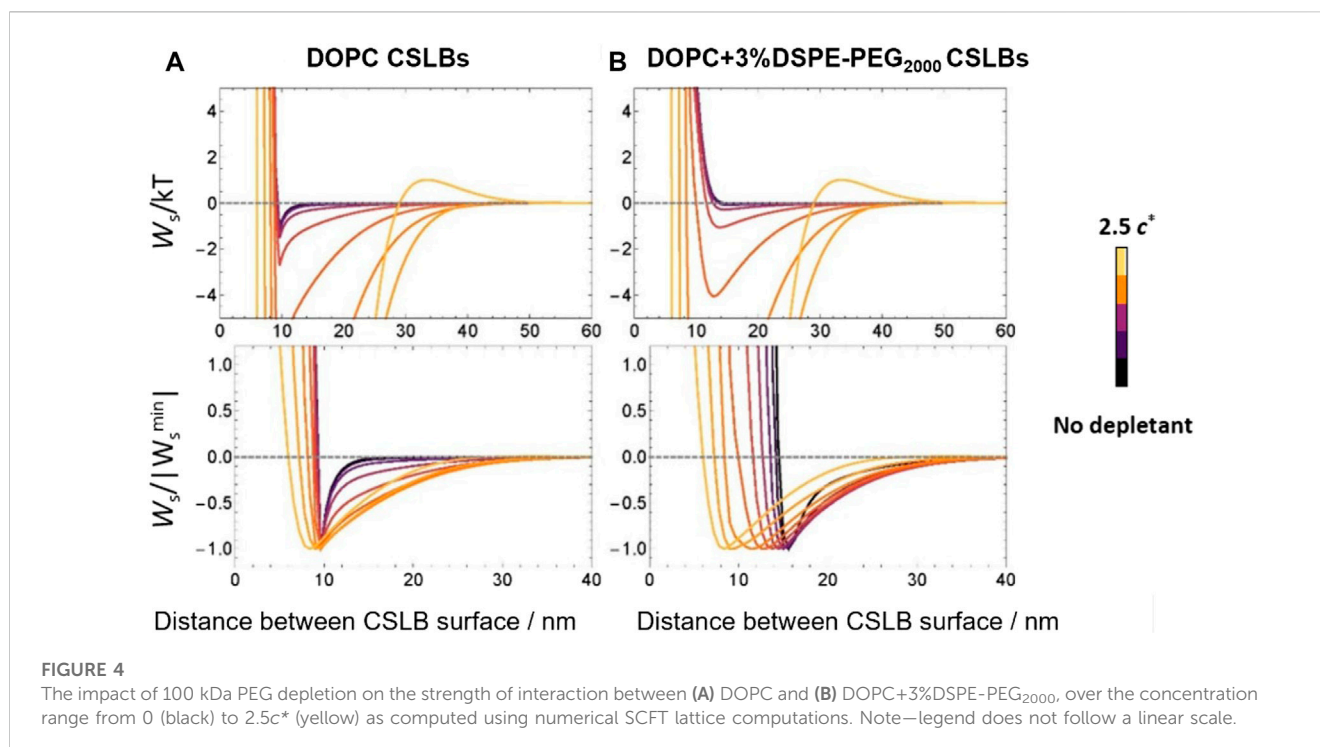
Figure 2A shows confocal microscopy images of DOPC and DPPC CSLBs with 0, 5 and 10%DSPE-PEG$_{2000}$ at high area fraction $\varphi = 0.11$. For clarity, the confocal microscopy images displayed in Figure 2A are a representative segment of the larger tilescan images analysed. It is apparent that clustering is significantly reduced when comparing confocal images of CSLBs with 0%–10% PEGylated lipid. This is most clear for the DPPC CSLBs, however, the precise configuration of particle clusters and quantification of the impact of PEGylated lipid on CSLB interaction is not possible to determine by eye. Therefore, using the image analysis approach described in ESI—Supplementary Section S6, the cluster distributions and $g(r)$ curves for CSLBs were determined (Figures 2B–D).

Figures 2B, C show that at low CSLB area fractions the addition of PEGylated lipid to the bilayer increases the number of single particles being present for both DOPC and DPPC CSLBs, indicating the effectiveness of the steric repulsion induced by the DSPE-PEG$_{2000}$. In compositions where 0 or 10% of DSPE-PEG$_{2000}$ are added to the bilayer, both DOPC and DPPC CSLBs show

FIGURE 4
The impact of 100 kDa PEG depletion on the strength of interaction between **(A)** DOPC and **(B)** DOPC+3%DSPE-PEG$_{2000}$, over the concentration range from 0 (black) to 2.5$c*$ (yellow) as computed using numerical SCFT lattice computations. Note—legend does not follow a linear scale.

comparable singlet stability, ~30% and ~65%, respectively. DPPC+5%DSPE-PEG$_{2000}$ CSLBs demonstrated the highest stability at 75% singlets. At high area fractions, again the impact of PEGylated lipid is apparent in increasing the number of single particles. The CSLBs composed of the gel lipid DPPC show systematically lower number of singlets than DOPC CSLBs, regardless of the DSPE-PEG$_{2000}$ concentration.

In general, at all area fractions singlets are the predominant cluster size for all investigated samples. Additionally, there appears to be a continuous decrease in the percentage of particles across the cluster sizes, with the sharpest decrease seen in samples with PEGylated lipid in the membrane (Figures 2B, C). DPPC and DOPC CSLBs without PEGylated lipid demonstrated a more gradual decrease as they tended to be more clustered already at low area fractions.

Comparing the $g(r)$ characteristics of DOPC and DPPC CSLBs, with and without PEGylated lipids, allows for quantitative evaluation of how the type and phase state (fluid or gel like) of the main phospholipid affect the interaction strength in the colloidal system (Figure 2D). Here we focus on the interactions of fluid and gel CSLBs at high area fraction φ = 0.11. For each membrane composition the first $g(r)$ peak occurred at r = 3 μm, and as expected all $g(r)$ curves can be seen tending to 1 for large r. DPPC CSLBs with no PEGylated lipid demonstrated consistently a higher first peak at r = 3 μm than DOPC CSLBs, indicating a stronger attraction at that proximity (Figures 2C, D). Additionally, regardless of DSPE-PEG$_{2000}$ concentration, gel DPPC CSLBs were seen to invariably have higher first peaks, therefore stronger interactions, than the DOPC CSLBs (Figure 2D). All samples also demonstrated a second peak at r = 6, the more pronounced being the DPPC CSLBs (Figure 2D, first panel). Visually this can be reconciled by comparing the confocal microscopy images in Figure 2A where dense, defined clusters are more obvious for DPPC CSLBs than for DOPC CSLBs.
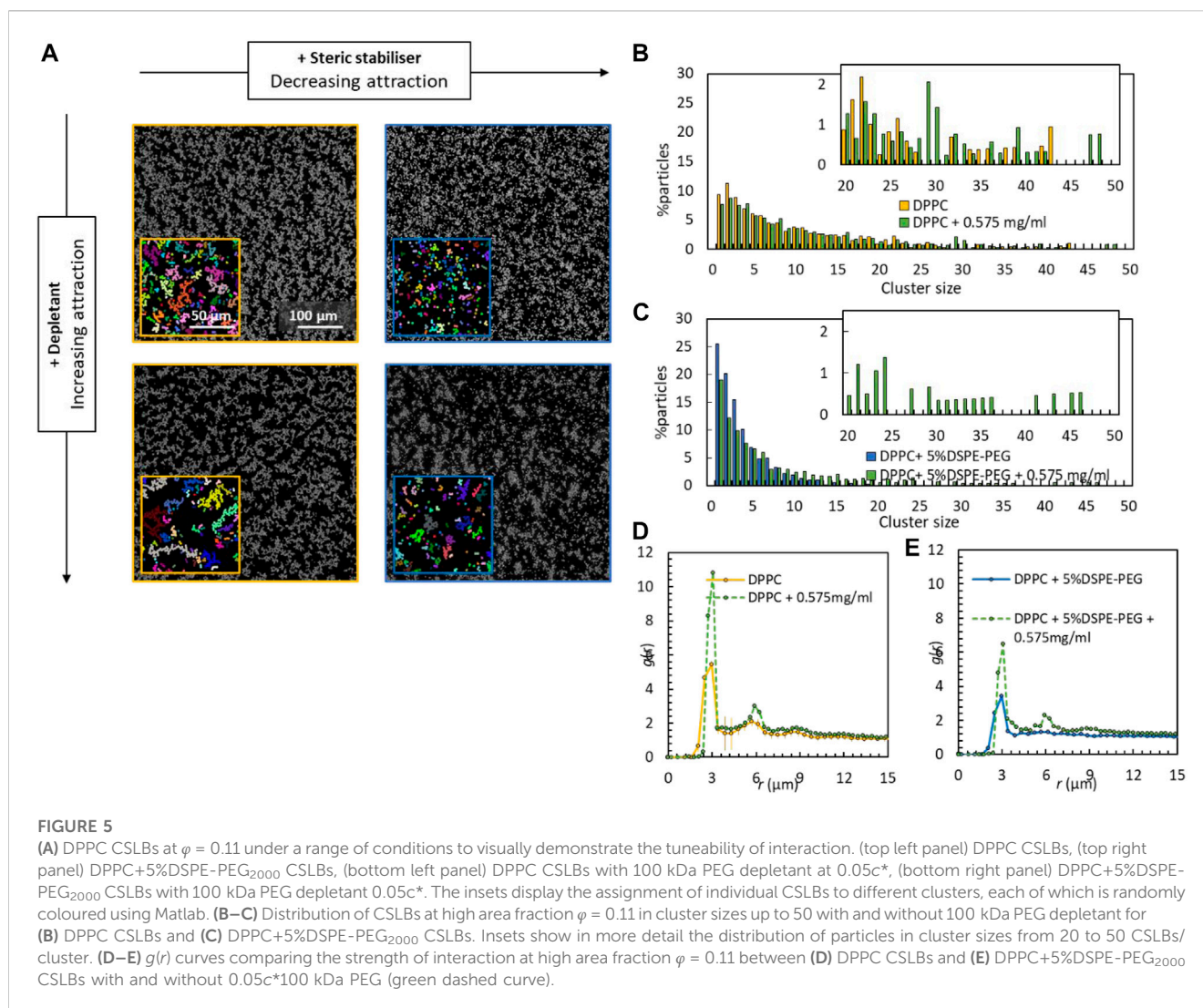
Overall, from these results it appears that for both DOPC and DPPC CSLBs, membranes composed of 5%DSPE-PEG2000 show the lowest attractive interaction. Additionally, it is known that the membrane of DOPC+5%DSPE-PEG$_{2000}$ CSLBs remains fluid, while DPPC+5%DSPE-PEG$_{2000}$ CSLBs are gel (Giakoumatos et al., 2022) This indicates that DOPC+5%DSPE-PEG$_{2000}$ and DPPC+5%DSPE-PEG$_{2000}$ CSLB compositions are optimal for further studies where both colloidal stability and contrasting membrane fluidity are required.

Modulating CSLB interactions *via* depletion forces

Now that we have shown that the colloidal stability of the CSLBs can be improved by adding PEGylated lipids to the membrane to induce steric repulsion, it is interesting to test the boundaries of this colloidal stability. Furthermore, to consider if CSLBs could be suitable in applications such as sensing, wherein more complex media such as serum may be unavoidable, it is important to check how robust the stability of the system is in the presence of free (macro)molecules. To this end, we supplement our CSLB dispersion with a non-adsorbing polymer, 100 kDa PEG, by which we induce an attractive depletion interaction (de Hoog et al., 2001; Lu et al., 2008; Lekkerkerker and Tuinier, 2011a).

Theoretical prediction of depletion forces on colloid supported lipid bilayers

First we apply SCFT computations to elucidate the way in which the PEG depletant interacts with the CSLBs: by depletion from the bilayer or by penetration close to the silica surface (Figure 3, ESI—Supplementary Section S1). For bare silica particles, the

FIGURE 5
(A) DPPC CSLBs at φ = 0.11 under a range of conditions to visually demonstrate the tuneability of interaction. (top left panel) DPPC CSLBs, (top right panel) DPPC+5%DSPE-PEG$_{2000}$ CSLBs, (bottom left panel) DPPC CSLBs with 100 kDa PEG depletant at 0.05c*, (bottom right panel) DPPC+5%DSPE-PEG$_{2000}$ CSLBs with 100 kDa PEG depletant 0.05c*. The insets display the assignment of individual CSLBs to different clusters, each of which is randomly coloured using Matlab. **(B–C)** Distribution of CSLBs at high area fraction φ = 0.11 in cluster sizes up to 50 with and without 100 kDa PEG depletant for **(B)** DPPC CSLBs and **(C)** DPPC+5%DSPE-PEG$_{2000}$ CSLBs. Insets show in more detail the distribution of particles in cluster sizes from 20 to 50 CSLBs/cluster. **(D–E)** $g(r)$ curves comparing the strength of interaction at high area fraction φ = 0.11 between **(D)** DPPC CSLBs and **(E)** DPPC+5%DSPE-PEG$_{2000}$ CSLBs with and without 0.05c*100 kDa PEG (green dashed curve).

depletant PEG can closely approach the particle surface, but it forms a depletion zone due to entropy loss (Figure 3A).

For DOPC CSLBs and DOPC + DSPE-PEG$_{2000}$ CSLBs, the segment concentration profile of the PEG depletant shifts away from the particle surface by approximately 5 nm, which corresponds to the thickness of the lipid bilayer (Figures 3B, C) (Gumí-Audenis et al., 2015; Gumí-Audenis et al., 2016). Furthermore, the impact of depletion forces on the strength of the interactions between CSLBs was computed by SCFT for depletant concentrations ranging from 0 to 2.5c*, where c* determines the critical overlap concentration (Figure 4, ESI—Supplementary Section S11).

SCFT elucidates a strong trend of increasing attraction mediated by non-adsorbing PEG chains between both DOPC and DPPC CSLBs upon addition of depletant, regardless of membrane stabiliser DSPE-PEG$_{2000}$ inclusion (Figures 4A, B). This indicates that the interactions between CSLBs can be tuned by multiple handles, specifically here by including stabiliser and by introducing depletion forces. Note that a (modest) repulsive contribution to the interaction between the CSLBs is found around an interparticle distance of 30 nm (Figure 4A) for the highest free PEG concentration added [ESI (Mao et al., 1995; Semenov and Shvets,

2015)] However, the attraction at shorter interparticle distances still overwhelms this weak repulsion.

Quantifying the impact of depletion forces on colloid supported lipid bilayers

By varying the amount of free polymer, the effective range and strength of the attraction between colloids can be modified.[15] The polymer overlap concentration (c*) quantifies the point at which a polymer solution moves from the dilute regime, where single polymer chains do not interact with one another, to the semi-dilute or entanglement regime (ESI—Supplementary Section S11). Additionally, c*gives the concentration beyond which the addition of extra polymer will start to have a less significant effect on the strength of depletion.[30] For this study, we select concentrations corresponding to 0.05c* being 0.575 mg/mL. It is expected that the addition of depletant to the CSLB dispersion at the concentrations chosen would exacerbate the occurrence of dense, defined CSLB clusters, such as those seen for DPPC CSLBs at high area fractions (Lekkerkerker and Tuinier, 2011b).
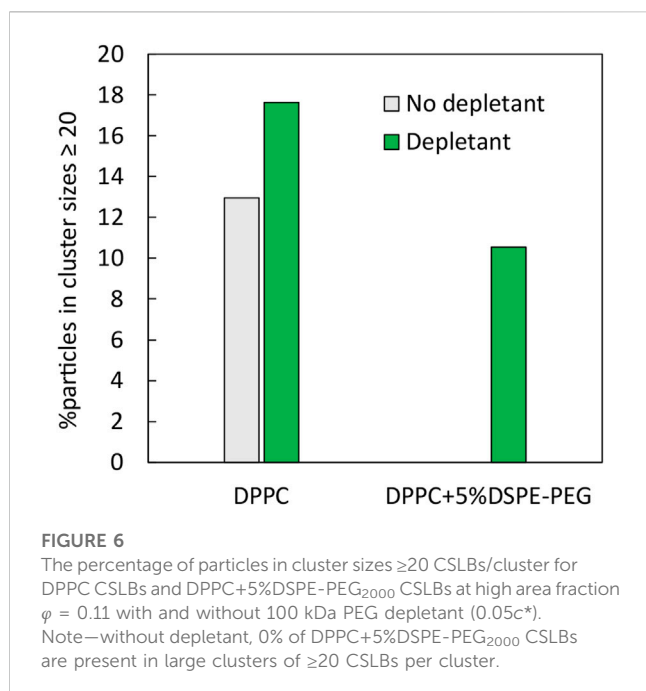
FIGURE 6
The percentage of particles in cluster sizes ≥20 CSLBs/cluster for
DPPC CSLBs and DPPC+5%DSPE–PEG$_{2000}$ CSLBs at high area fraction
φ = 0.11 with and without 100 kDa PEG depletant (0.05c*).
Note—without depletant, 0% of DPPC+5%DSPE–PEG$_{2000}$ CSLBs
are present in large clusters of ≥20 CSLBs per cluster.

Figure 5 displays the results of confocal imaging and subsequent data analysis for DPPC and DPPC+5%DSPE-PEG$_{2000}$ CSLBs at a fixed PEG depletant concentration 0.05c*. These dispersions were selected as illustrative cases for systems with high and low interaction strength, respectively. The effect of steric stabilisation by DSPE-PEG$_{2000}$ as well as the impact of the additional attraction due to the polymer depletant 100 kDa PEG on the colloidal stability of the CSLBs are clearly visible (Figure 5A).

DPPC CSLBs without stabilizer assemble into numerous dense clusters of a ramified, elongated shape and generate a space filling network (Figure 5A. Top left). This is indicative of a significant attraction between the CSLBs, which leads to fractal aggregation until the aggregates touch (de Hoog et al., 2001; Anderson and Lekkerkerker, 2002). Upon the addition of depletant, this elongated shape is even more pronounced. Larger and more well-defined clusters appear indicating gelation by arrested spinodal phase separation (Figure 5A, bottom left) (de Hoog et al., 2001; Lu et al., 2008).

By contrast, the DPPC CSLBs with 5%DSPE-PEG$_{2000}$ stabilizer are well distributed (Figure 5A top right). Small clusters and single particles are predominant. The addition of depletant destabilizes the dispersion, which now also contains larger clusters (Figure 5A bottom-right). A noticeable number of singlets and small aggregates remains. The larger clusters appear somewhat smaller and less heterogeneous in dimensions and shape than those observed for DPPC CSLBs with (out) depletant. Presumably, the aggregates are able to reorganise, possibly as a consequence of the additional steric stabilization afforded by the PEGylated lipid. We suspect that the larger clusters accumulate at the expense of the small clusters or single CSLBs, such as by nucleation and growth (de Hoog et al., 2001). A future time-resolved imaging study could test our conjecture and reveal whether both dispersions are indeed at 0.05c* depletant in a two-phase regime of the state diagram, wherein the larger aggregates form *via* spinodal decomposition or *via* nucleation and growth, as hypothesized for the DPPC CSLBs without stabilizer

and the DPPC CSLBs with 5% DSPE-PEG$_{2000}$ stabilizer, respectively.

Interestingly, the cluster distributions (calculated for clusters up to 50 CSLBs per cluster) reveal a predominance of clusters in all systems (Figures 5B, C). More than 97% of all particles reside in clusters composed of 50 CSLBs or smaller. The clusters are smallest in the most stable dispersion (DPPC+5%DSPE-PEG$_{2000}$ CSLBs) without depletant, wherein 100% of the particles reside in clusters composed of less than 20 CSLBs. Regardless of the presence of the stabilizer, more particles end up in larger aggregates under the influence of added depletant (Figure 6). For example, without depletion, no clusters larger than 19 particles are detected in suspensions of DPPC+5%DSPE-PEG$_{2000}$ CSLBs, whilst under the influence of depletion, more than 10% of CSLBs are found in clusters of 20 particles or larger.

Next, the strength of attraction between the CSLBs under the influence of depletion was evaluated *via* analysis of the radial distribution functions (Figures 5D, E). The addition of depletant results in an increase in the height of the first two peaks and a narrowing of the second peak for CSLBs with and without stabilizer. Additional peaks at $r = 9$ (and in some cases 12 μm) are also more pronounced in the presence of the depletant than in its absence. All of these observations underline a substantial increase in attraction between the CSLBs upon addition of depletant, as predicted by SCFT. As expected, the strongest attraction occurs between DPPC CSLBs under the influence of depletant. The next predominant attraction occurs in DPPC+5%DSPE-PEG$_{2000}$ CSLBs with depletant, closely followed by DPPC CSLBs without depletant. CSLBs of DPPC+5%DSPE-PEG$_{2000}$ CSLBs without depletant are least attractive. These results unambiguously demonstrate that the attraction between CSLBs can be modulated by PEGylation and/or addition of depletants. Not only is it possible to induce stability and reduce attraction between DPPC CSLBs by incorporation of a PEGylated lipid into the bilayer, but it is also possible to strengthen the attraction *via* depletion.

Conclusion

In this study, the influence of membrane fluidity, stabilizer and depletant on colloidal stability of and interactions between colloid supported lipid bilayers (CSLB) was investigated experimentally and computationally. CSLBs were prepared from fluid-like DOPC and gel-like DPPC phospholipids to examine the impact of membrane fluidity. PEGylated lipids were introduced in the membranes and polymeric depletants in the medium to probe the tuneability of the interactions between the CSLBs. Without membrane bound DSPE-PEG$_{2000}$, both types of CSLBs showed significant clustering and attraction. The addition of 5 mol% DSPE-PEG$_{2000}$ induced a profound increase in stability. Further addition of stabilizer up to 10% DSPE-PEG$_{2000}$ led to minimal variations in stability, while the interaction strength slightly increased in comparison to DOPC and DPPC CSLBs with 5% DSPE-PEG$_{2000}$. Dispersions were supplemented with 100 kDa PEG to impose depletion forces on DPPC CSLBs without stabilizer and with 5% DSPE-PEG$_{2000}$. In line with the SCFT predictions, this destabilized the colloidal system further and modulated the strength of attraction. Aggregates of various size and density formed. Under certain conditions these evolved into space filling networks, transforming the colloidal

dispersions into gels. Aiming to assess colloidal stability and interparticle interactions in a quantitative fashion, we analysed cluster distributions and radial distribution functions obtained from confocal images taken under different conditions at a fixed time point after sample preparation. The cluster distributions under non-arrested conditions will likely coarsen over time. A complementary kinetic study could monitor this phenomenon over time and shed further light on the mechanisms of aggregation, gelation and arrest. Interestingly, the least prominent attractive interaction at both low and high particle concentrations is observed for CSLBs with 5%DSPE-PEG2000 in the fluid-like DOPC or the gel-like DPPC. These particles are thus suitable candidates for further studies in which both colloidal stability and contrasting membrane fluidity are required.

Data availability statement

The original contributions presented in the study are included in the article/Supplementary Material, further inquiries can be directed to the corresponding author.

Author contributions

ECG, BGA and IKV conceived the experiments. ECG and BGA performed the experiments. ECG, BGA, LSH, and HF performed the data analysis. AGG performed and analysed the simulations. IKV and RT supervised the research. The manuscript was written with contributions from all authors.

Conflict of interest

The authors declare that the research was conducted in the absence of any commercial or financial relationships that could be construed as a potential conflict of interest.

Publisher's note

All claims expressed in this article are solely those of the authors and do not necessarily represent those of their affiliated organizations, or those of the publisher, the editors and the reviewers. Any product that may be evaluated in this article, or claim that may be made by its manufacturer, is not guaranteed or endorsed by the publisher.

Supplementary material

The Supplementary Material for this article can be found online at: https://www.frontiersin.org/articles/10.3389/frsfm.2023.1110297/full#supplementary-material

References

Anderson, V. J., and Lekkerkerker, H. N. W. (2002). Insights into phase transition kinetics from colloid science. *Nature* 416, 811–815. doi:10.1038/416811a

Bergman, M. (2019). On the phase behaviour of soft matter: understanding complex interactions via quantitative imaging. https://portal.research.lu.se/en/publications/on-the-phase-behaviour-of-soft-matter-understanding-complex-inter.

Chakraborty, I., Meester, V., van der Wel, C., and Kraft, D. J. (2017). Colloidal joints with designed motion range and tunable joint flexibility. *Nanoscale* 9, 7814–7821. doi:10.1039/C6NR08069C

de Hoog, E. H. A., Kegel, W. K., van Blaaderen, A., and Lekkerkerker, H. N. W. (2001). Direct observation of crystallization and aggregation in a phase-separating colloid-polymer suspension. *Phys. Rev. E* 64, 21407. doi:10.1103/PhysRevE.64.021407

Devanand, K., and Selser, J. C. (1991). Asymptotic behavior and long-range interactions in aqueous solutions of poly(ethylene oxide). *Macromolecules* 24, 5943–5947. doi:10.1021/ma00022a008

Fleer, G. J., Cohen Stuart, M. A., Scheutjens, J. M. H. M., Cosgrove, T., and Vincent, B. (1993). *Polymers At Interfaces*. Heidelberg, Germany: springer.

Fleer, G. J. (2010). Polymers at interfaces and in colloidal dispersions. *Adv. Colloid Interface Sci.* 159, 99–116. doi:10.1016/j.cis.2010.04.004

Garbuzenko, O., Barenholz, Y., and Priev, A. (2005). Effect of grafted PEG on liposome size and on compressibility and packing of lipid bilayer. *Chem. Phys. Lipids* 135, 117–129. doi:10.1016/j.chemphyslip.2005.02.003

Giakoumatos, E. C., Gascoigne, L., Gumí-Audenis, B., García, A. G., Tuinier, R., and Voets, I. K. (2022). Impact of poly(ethylene glycol) functionalized lipids on ordering and fluidity of colloid supported lipid bilayers. *Soft Matter* 18, 7569–7578. doi:10.1039/D2SM00806H

González García, Á., Ianiro, A., Beljon, R., Leermakers, F. A. M., and Tuinier, R. (2020). (Homo)polymer-mediated colloidal stability of micellar solutions. *Soft Matter* 16, 1560–1571. doi:10.1039/C9SM01665A

González García, Á., Timmers, E. M., Romijn, N., Song, S., Sahebali, S., Tuinier, R., et al. (2019). Micellization of a weakly charged surfactant in aqueous salt solution: Self-

consistent field theory and experiments. *Colloids Surfaces A Physicochem. Eng. Aspects* 561, 201–208. doi:10.1016/j.colsurfa.2018.10.039

Gumí-Audenis, B., Costa, L., Carlá, F., Comin, F., Sanz, F., and Giannotti, M. (2016). Structure and nanomechanics of model membranes by atomic force microscopy and spectroscopy: Insights into the role of cholesterol and sphingolipids. *Membranes* 6, 58. doi:10.3390/membranes6040058

Gumí-Audenis, B., Sanz, F., and Giannotti, M. I. (2015). Impact of galactosylceramides on the nanomechanical properties of lipid bilayer models: An AFM-force spectroscopy study. *Soft Matter* 11, 5447–5454. doi:10.1039/C5SM01252J

Hill, T. L. (1986) *An introduction to statistical thermodynamics*, 2nd ed. Dover Publications, New York, NY, USA

Ianiro, A., González García, Á., Wijker, S., Patterson, J. P., Esteves, A. C. C., and Tuinier, R. (2019). Controlling the spatial distribution of solubilized compounds within copolymer micelles. *Langmuir* 35, 4776–4786. doi:10.1021/acs.langmuir.9b00180

Ianiro, A., Patterson, J., González García, Á., van Rijt, M. M. J., Hendrix, M. M. R. M., Sommerdijk, N. A. J. M., et al. (2018). A roadmap for poly(ethylene oxide)-block -poly-ε-caprolactone self-assembly in water: Prediction, synthesis, and characterization. *J. Polym. Sci. Part B Polym. Phys.* 56, 330–339. doi:10.1002/polb.24545

Ivell, S. J., Dullens, R. P. A., Sacanna, S., and Aarts, D. G. A. L. (2013). Emerging structural disorder in a suspension of uniformly dimpled colloidal particles. *Soft Matter* 9, 9361–9365. doi:10.1039/C3SM52059E

Lauw, Y., Leermakers, F. A. M., and Cohen Stuart, M. A. (2006). Self-Consistent-Field Analysis of the Micellization of Carboxy-Modified Poly(ethylene oxide)−poly(propylene oxide)−poly(ethylene oxide) Triblock Copolymers. *J. Phys. Chem. B* 110, 465–477. doi:10.1021/jp053795a

Leermakers, F., Eriksson, J. C., and Lyklema, J. (2005). "Association colloids and their equilibrium modelling," in *Fundamentals of interface and colloid science* (Amsterdam, Netherlands: Elsevier), 1–4. doi:10.1016/s1874-5679(05)80008-x

Lekkerkerker, H. N. W., and Tuinier, R. (2011). *Colloids and the depletion interaction*. Heidelberg, Germany: Springer Science.

Lekkerkerker, H. N. W. W., and Tuinier, R. (2011). *Colloids and the depletion interaction*. Dordrecht, Netherlands: Springer.

Li, F., Marcelis, A. T. M., Sudhölter, E. J. R., Cohen Stuart, M. A., and Leermakers, F. A. M. (2009). Field theoretical modeling of the coexistence of micelles and vesicles in binary copolymer mixtures. *Soft Matter* 5, 4173–4184. doi:10.1039/B904525B

Lu, P. J., Zaccarelli, E., Ciulla, F., Schofield, A. B., Sciortino, F., and Weitz, D. A. (2008). Gelation of particles with short-range attraction. *Nature* 453, 499–503. doi:10.1038/nature06931

Mao, Y., Cates, M. E., and Lekkerkerker, H. N. W. (1995). Depletion force in colloidal systems. *Phys. A Stat. Mech. its Appl.* 222, 10–24. doi:10.1016/0378-4371(95)00206-5

Meijer, L. A., Leermakers, F. A. M., and Lyklema, J. (1995). Modeling the interactions between phospholipid bilayer membranes with and without additives. *J. Phys. Chem.* 99, 17282–17293. doi:10.1021/j100047a037

Moerman, P. (2019). *Dynamics of active droplets and freely jointed colloidal trimers*. Utrecht, Netherlands: Utrecht University.

Needham, D., and Kim, D. H. (2000). PEG-Covered lipid surfaces: Bilayers and monolayers. *Colloids Surfaces B Biointerfaces* 18, 183–195. doi:10.1016/S0927-7765(99)00147-2

Philipse, A. P., Tuinier, R., Kuipers, B. W. M., Vrij, A., and Vis, M. (2017). On the repulsive interaction between strongly overlapping double layers of charge-regulated surfaces. *Colloid Interface Sci. Commun.* 21, 10–14. doi:10.1016/j.colcom.2017.10.002

Poon, W., Pusey, P., and Lekkerkerker, H. (1996). Colloids in suspense. *Phys. World* 9, 27–34. doi:10.1088/2058-7058/9/4/23

Pyrkova, D. V., Tarasova, N. K., Pyrkov, T. V., Krylov, N. A., and Efremov, R. G. (2011). Atomic-scale lateral heterogeneity and dynamics of two-component lipid bilayers composed of saturated and unsaturated phosphatidylcholines. *Soft Matter* 7, 2569–2579. doi:10.1039/C0SM00701C

Rinaldin, M., Fonda, P., Giomi, L., and Kraft, D. J. (2020). Geometric pinning and antimixing in scaffolded lipid vesicles. *Nat. Commun.* 11, 4314. doi:10.1038/s41467-020-17432-w

Rinaldin, M., Verweij, R. W., Chakraborty, I., and Kraft, D. J. (2019). Colloid supported lipid bilayers for self-assembly. *Soft Matter* 15, 1345–1360. doi:10.1039/c8sm01661e

Royall, C. P., Leunissen, M. E., and Blaaderen, A. (2003). A new colloidal model system to study long-range interactions quantitatively in real space. *J. Phys. Condens. Matter* 15, S3581–S3596. doi:10.1088/0953-8984/15/48/017

Scheutjens, J. M. H. M., and Fleer, G. J. (1979). Statistical theory of the adsorption of interacting chain molecules. 1. Partition function, segment density distribution, and adsorption isotherms. *J. Phys. Chem.* 83, 1619–1635. doi:10.1021/j100475a012

Scheutjens, J. M. H. M., and Fleer, G. J. (1980). Statistical theory of the adsorption of interacting chain molecules. 2. Train, loop, and tail size distribution. *J. Phys. Chem.* 84, 178–190. doi:10.1021/j100439a011

Semenov, A. N., and Shvets, A. A. (2015). Theory of colloid depletion stabilization by unattached and adsorbed polymers. *Soft Matter* 11, 8863–8878. doi:10.1039/C5SM01365H

Stenkamp, V. S., and Berg, J. C. (1997). The role of long tails in steric stabilization and hydrodynamic layer thickness. *Langmuir* 13, 3827–3832. doi:10.1021/la970173a

Tribet, C., and Vial, F. (2008). Flexible macromolecules attached to lipid bilayers: Impact on fluidity, curvature, permeability and stability of the membranes. *Soft Matter* 4, 68–81. doi:10.1039/B708431P

van der Meulen, S. A. J., Helms, G., and Dogterom, M. (2015). Solid colloids with surface-mobile linkers. *J. Phys. Condens. Matter* 27, 233101. doi:10.1088/0953-8984/27/23/233101

van der Meulen, S. A. J., and Leunissen, M. E. (2013). Solid colloids with surface-mobile DNA linkers. *J. Am. Chem. Soc.* 135, 15129–15134. doi:10.1021/ja406226b

Whitmer, J. K., and Luijten, E. (2011). Sedimentation of aggregating colloids. *J. Chem. Phys.* 134. doi:10.1063/1.3525923

Yethiraj, A., and van Blaaderen, A. (2003). A colloidal model system with an interaction tunable from hard sphere to soft and dipolar. *Nature* 421, 513–517. doi:10.1038/nature01328